ELSEVIER

Journal of Power Sources 52 (1994) 211–216

JOURNAL OF POWER SOURCES

A quick method of measuring the capacity versus discharge rate for a dual lithium-ion insertion cell undergoing cycling

Marc Doyle [a], John Newman [a], Jan Reimers [b]

[a] *Energy and Environment Division, Lawrence Berkeley Laboratory and Department of Chemical Engineering, University of California, Berkeley, CA 94720, USA*

[b] *Moli Energy (1990) Limited, Maple Ridge, BC, V2X 9E7, Canada*

Received 25 April 1994; accepted in revised form 3 August 1994

Abstract

During extended cycling of an experimental cell, it is common to test periodically the rate behaviour of the cell by performing a series of discharges at various rates and measuring the capacity to a cutoff potential. The fastest way to obtain this information is to carry out successive discharges at decreasing rates with a brief relaxation period between each discharge but no charging step. The capacity obtained at a given rate is assumed to be the cumulative capacity up to that point. We have simulated this testing procedure to determine when the method is valid and have developed criteria for the optimum number of discharges and relaxation times to use. It is found that a series of seven discharges with a 5 min relaxation period gives an accurate prediction of the cell capacity with less than 1% error. The mechanisms which cause erroneous results to arise are described. The system chosen for simulation is the Li_xC_6|propylene carbonate +1 M $LiClO_4$|$Li_yMn_2O_4$ dual lithium-ion insertion cell. Experimental discharge curves are provided that verify the results of the simulations.

Keywords: Capacity; Discharge rate; Lithium-ion insertion cell; Cycling

1. Introduction

The dual lithium-ion insertion ('rocking-chair') cell uses materials with differing chemical potentials for the inserted lithium in the two hosts. The high energy density and inherent reversibility of insertion reactions makes them ideal for rechargeable battery electrodes. The primary advantage of the lithium-ion insertion cell is its improvement in safety over cells using solid lithium as the negative electrode. Batteries based on this concept have recently begun reaching the consumer market, and lithium-ion electric-vehicle batteries are being considered.

The process of scaling up a cell necessarily involves extended cycling of many thousands of cells before the optimum design parameters are established. This process is expensive both in terms of time and materials, and the main task of modelling and computer simulation is to reduce some of this expense. During cycling it is common to determine periodically the rate behaviour of a cell by interrupting the cycling to perform a series of discharges at various rates, each followed by a charging step and a relaxation period. The capacity of the cell as a function of discharge rate is thus obtained. This information is useful for identifying losses in reversible capacity over time (very-low-rate capacity) as well as the peak-power availability (very-high-rate capacity). Depending on the number of data points taken and the frequency with which this procedure is carried out, obtaining this information may be as time consuming as the extended cycling itself.

A less time-consuming method of obtaining the capacity versus discharge rate for a dual lithium-ion battery has been suggested and used successfully at Moli Energy. The procedure is to carry out successive discharges of the cell to a cutoff potential starting with the highest rate and followed by ever decreasing rates. Each discharge is preceded by a brief relaxation period but not a charging step. The capacity obtained at a given rate is assumed to correspond to the cumulative capacity up to that time. This method takes substantially less time than that of a single low-rate discharge of the cell, because most of the cell's capacity is consumed with the higher-rate discharges. Although this method has been used in the past to measure the capacity of other non-lithium-based battery systems, we are not

SSDI 0378-7753(94)02012-R

aware of any attempt to examine the validity of the method from a theoretical perspective.

In this paper we attempt to use computer simulations to gauge the reliability and validity of the above method. We seek to determine the optimum procedure to use to ensure that the results obtained are valid, including how many data points and how much relaxation time is sufficient. We also explore the phenomena occurring inside the cell which can cause this method to give erroneous results. Although the simulation results are for one particular system, our conclusions are generalized to apply to any system.

We have developed mathematical models of lithium-based cells; the details of these models can be found elsewhere [1,2]. In earlier work, computer simulations were used to identify the phenomena that limit the high-rate discharge of the lithium/polymer cell and the lithium-ion insertion cell. More recently, we have used the models to explore lithium cells with a unity transference number for the lithium ion [3]. Our work attempts to demonstrate the utility of detailed mathematical modelling in the development of new battery systems.

2. Results and discussion

Appendix A gives the transport properties for the electrolyte and thermodynamic data for each electrode. We modelled a cell consisting of a carbon negative electrode, lithium perchlorate in a propylene carbonate liquid electrolyte, and a lithium–manganese-oxide spinel positive electrode. The lithium perchlorate/propylene carbonate electrolyte in the separator region of the cell is confined to the voids of an inert polymer material such as polypropylene. The inert separating material is assumed to have a constant void fraction of 0.38, and transport properties of the electrolyte in this region are adjusted accordingly.

Additional parameters used in these simulations are listed in Table 1. No attempt has been made to optimize the materials or design parameters for the cell being simulated; rather, these choices are based on availability of data and similarity to systems described in the literature [4,5]. The maximum concentrations in the positive and negative electrodes are estimated from the density and mol. wt. of the material at composition $LiMn_2O_4$ or LiC_6, respectively. The state-of-charge is measured with y, the stoichiometry of the positive electrode ($Li_yMn_2O_4$). The lithium–manganese-oxide spinel electrode is assumed to insert lithium over the range ($0.2 < y < 1.0$); hence, the initial solid concentration is 20% of the total, or maximum, concentration. The carbon material is petroleum coke, with the composition range for lithium insertion being $0 < x < 0.495$ in Li_xC_6. For this system, during charge, y varies between 1 and 0.2, and x varies between 0 and 0.495. The values of the electrode thicknesses and porosities are chosen such that the capacities of the two electrodes are balanced. The cell as described has a capacity of 20.1 C/cm^2; we shall refer to the capacity of the cell in terms of the utilization of positive electrode active material, as these quantities are directly related.

Table 1
System properties and design adjustable parameters

Parameter	$Li_yMn_2O_4$	Li_xC_6
D_s (cm^2 s^{-1})	10^{-9} [4]	5.0×10^{-9} [4]
σ (S cm^{-1})	1.0	1.0
i_0 (mA cm^{-2})	0.289 [a]	0.041 [a]
α_c, α_a	0.5	0.5
c_t (mol dm^{-3})	23.72	26.40
ρ_s (g cm^{-3})	4.1	1.9
δ_+, δ_- (μm)	200	243
R_s (μm)	1	18
c_s^0 (mol dm^{-3})	4.744	13.07
ϵ	0.3	0.3
ϵ_f	0.151	0.044
Parameter	**Value**	
T (°C)	25	
c^0 (mol dm^{-3})	1.00	
δ_s (μm)	50	

[a] Assumed value at initial conditions.

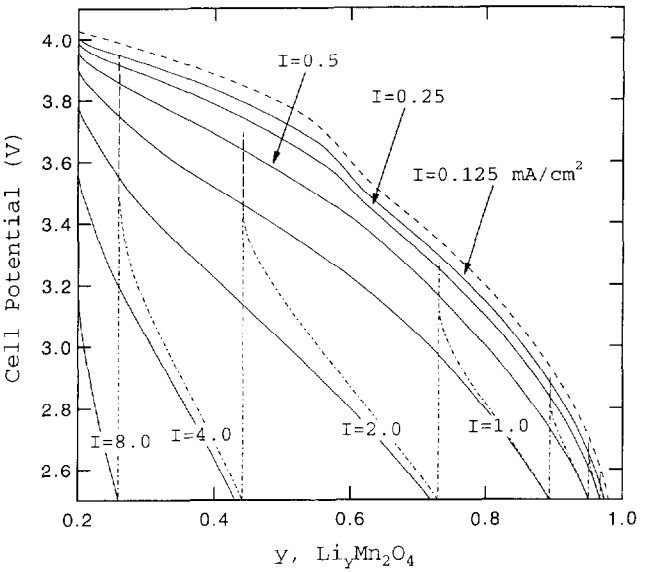

Fig. 1. Comparison of a signature curve (dotted line) with the individual separate discharge curves (solid lines). The cells are discharged to a 2.5 V cutoff potential. The dashed line is the open-circuit potential of the cell. Other parameters used in the simulations are given in Table 1.

Fig. 1 demonstrates two alternative methods for obtaining the capacity of a cell as a function of the discharge rate. Here we have first simulated the con-

stant-current discharge of the cell at various discharge rates to a cutoff potential of 2.5 V (solid lines). Each of these discharges starts from the same conditions, as if after each discharge the cell was recharged and then allowed to relax for a sufficient period of time. The dotted line gives the results of the faster method, consisting of first a very-high-rate discharge at $I=8.0$ mA cm^{-2} (to $y=0.26$), followed by a relaxation period of 30 min (vertical line). Next a discharge at $I=4.0$ mA cm^{-2} is performed, again followed by a 30 min relaxation period. This same procedure is repeated at discharge rates of $I=2.0$, 1.0, 0.5, 0.25 and 0.125 mA cm^{-2}. This dotted curve (Fig. 1) obtained has been termed a 'signature curve' for the cell. These two procedures provide the same information, the attainable capacity of the cell versus discharge rate, but the latter method takes less than a quarter of the time of the former.

A graph of the resulting capacity versus discharge rate is given in Fig. 2. Two sets of data are provided, consisting of discharges to either a 2.5 or a 3.0 V cutoff potential. The solid curve is obtained for comparison by carrying out many separate discharges similar to the solid lines in Fig. 1. The curves approach a maximum at low rates and would be expected eventually to reach zero capacity at a sufficiently large rate (for which the ohmic drop is large enough to cause the cell potential to fall below the cutoff potential instantaneously). The markers represent the results of signature curves identical to the above (Fig. 1) but with the time of relaxation between successive discharges as a parameter. Notice

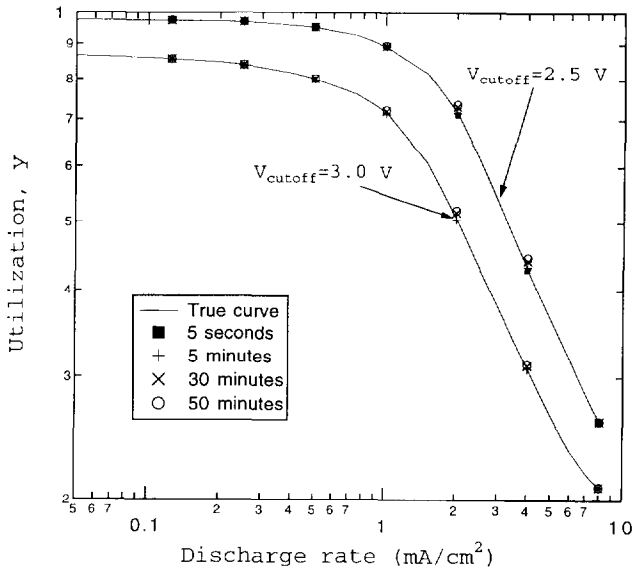

Fig. 2. A comparison of predictions of the capacity vs. the discharge rate for the carbon/manganese oxide spinel system. The solid curves are constructed from several separate discharges, while the markers are the predictions using the signature-curve method. The time of relaxation between discharges is a parameter. Other parameters used in the simulations are given in Table 1.

that the method appears to be relatively insensitive to the time allowed for relaxation. Even more interestingly, the method gives the best results for the smallest relaxation time. To understand this we must consider the processes that occur inside the cell while no current is being passed externally.

Since the subject of relaxation phenomena inside dual lithium-ion insertion cells has been discussed previously [6], we shall summarize only the relevant points. The two major processes that occur spontaneously are the relaxation of concentration gradients and the redistribution of lithium in the solid phases. The relaxation of concentration gradients, both of the salt in the solution phase and the lithium in the solid phase, has a relatively minor effect on a subsequent discharge of the cell. The redistribution of lithium in the active material, on the other hand, may be important. If a driving force exists, lithium can deinsert from one region of an electrode and insert into another region. The driving force, a difference in solid-phase open-circuit potential, must overcome the ohmic drop in solution, which depends on the distance between the two points. With insertion materials, where the open-circuit potential depends on the amount of lithium inserted, one will frequently find that there is a sufficient driving force to bring about a complete redistribution of lithium in the solid to a final uniform distribution.

Thus, the most important effect of the relaxation period is to give time for this redistribution process to occur. Slightly higher utilizations are found for two of the points in Fig. 2 (corresponding to $I=4$ and 2 mA cm^{-2}) for which 30 and 50 min of relaxation were allowed. This is because the redistribution of lithium in the active material which happened during these relaxation periods provided the subsequent discharge with more accessible unutilized active material at the front of the positive electrode. In addition, the higher-rate discharges are more sensitive to the redistribution of lithium because the ohmic drop is so much larger. The low-rate discharges, on the other hand, all appear in Fig. 2 to give the same capacities regardless of relaxation time. These points are relatively insensitive to the relaxation period because the time of discharge is much larger than that of the relaxation period.

We can examine this effect of the relaxation period in more detail by examining several signature curves having different relaxation times. In Fig. 3 we present simulated discharges corresponding to four different amounts of relaxation time: 5 s, 5 min, 30 min and 50 min. The time constant for the redistribution of active material can be estimated from [6]:

$$\tau=\frac{nF\rho_s\delta_+^2(1-\epsilon_+-\epsilon_{f,+})}{\kappa M_s(\mathrm{d}U/\mathrm{d}y)}$$

where the slope of the open-circuit potential with state-of-charge, $\mathrm{d}U/\mathrm{d}y$, can be obtained from expressions of

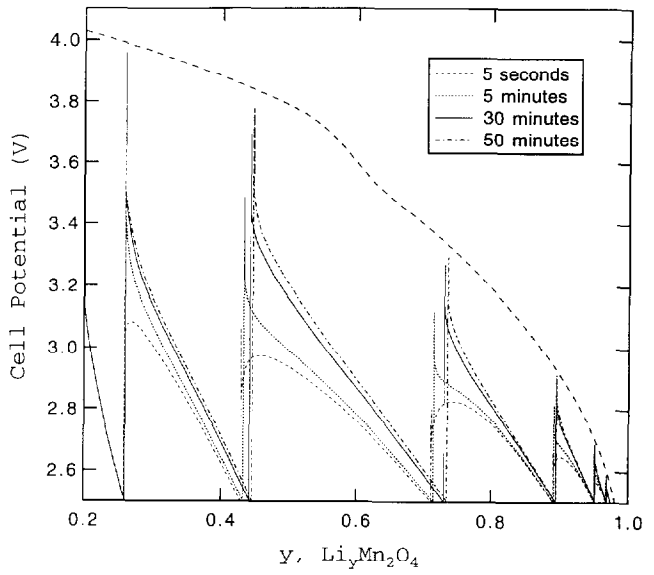

Fig. 3. Signature curves consisting of successive discharges to a cutoff potential of 2.5 V followed by relaxation periods where no current is passed. The time of relaxation between discharges is a parameter. The dashed line is the open-circuit potential of the cell. Other parameters used in the simulations are given in Table 1.

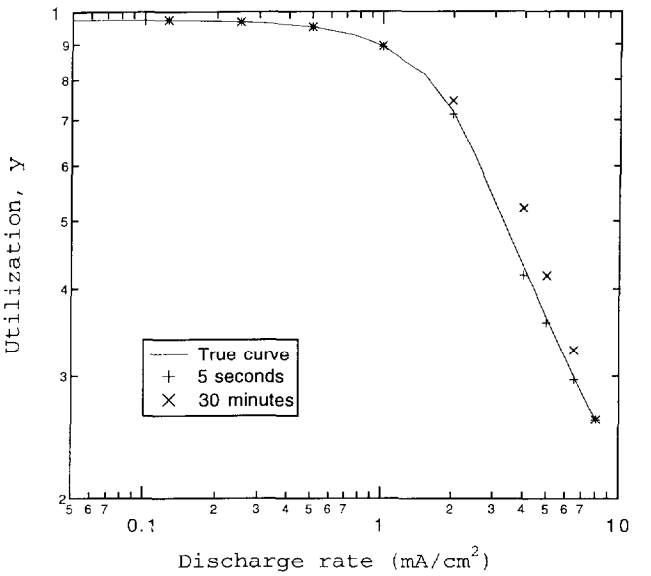

Fig. 4. The predicted capacity vs. discharge rate for the carbon/manganese oxide spinel system. The solid curve is obtained by carrying out many separate discharge. The data points are obtained with the signature-curve method. The time of relaxation is a parameter. The effect of using too many data points in the signature curve is demonstrated.

the form given in the Appendix (A1 or A2). We find that approximately 15 to 30 min are needed for this process to occur, the uncertainty coming from the need to choose a single slope to represent the open-circuit potential function for the lithium–manganese-oxide spinel. This explains why in Fig. 3 the curves for 5 s and 5 min appear to predict the same capacities while the curves for 30 and 50 min also appear to give the same capacities, though larger than the first pair. The short relaxation time used for the first two does not allow sufficient time for lithium to redistribute. The second pair of curves, on the other hand, reflects the material redistribution that has then had time to occur.

It is possible for the redistribution of lithium to have a major impact on the attainable capacity if too many data points at the higher discharge rates are used in the signature curve. In this situation the signature-curve method does not accurately predict the true capacity of the cell. As an example, we have used nine data points instead of the seven used previously, and placed these extra points at high discharge rates (6.5 and 5.0 mA cm^{-2}). The resulting predictions for capacity versus discharge rate are given in Fig. 4. Notice that the data points for a 30 min relaxation period vastly overestimate the capacity of the cell (21.2% error) while those for a 5 s relaxation period slightly underestimate the capacity (2.4% error). The high-rate data points are most sensitive to the relaxation period; using too many of them can result in large errors in the predicted capacity.

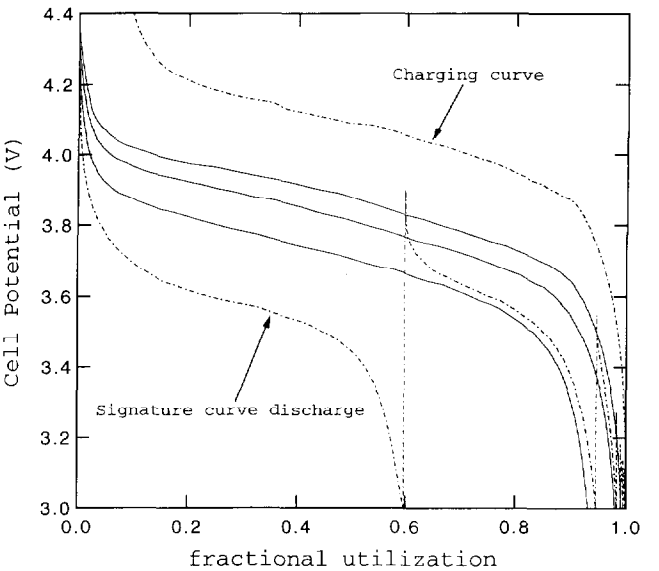

Fig. 5. Experimental data from a Moli Energy (1990) test cell. Comparison of predicted capacity from a signature curve (dotted line) with that of individual discharge curves (solid lines) at various rates. The capacity is normalized so that the utilization is based on the percentage of the maximum capacity. The discharge rates are given in the text.

All of the results presented above have come from computer simulations. As a final verification of the validity of the signature curve method, Fig. 5 gives a comparison of an experimental signature curve and three individual discharge curves from the same cell

to a 3.0 V cutoff potential. The data are taken from a Moli Energy test cell. This cell was not identical to the one simulated but does suit our purpose of demonstrating the accuracy of this method. The capacity is measured as the fraction of the maximum attainable capacity. Fig. 5 is similar to the simulation results given in Fig. 1; the dotted line is the signature curve and the solid lines are individual discharge curves. Note that the signature curve includes seven different discharges to the 3.0 V cutoff at decreasing rates and then a single charge back to the initial conditions. Only three of the individual discharge curves used for comparison with the signature curve are shown in Figs. 5 and 6; these are at the 1.0, 0.5, and 0.25 A rates. The capacities predicted by the signature curve are within 1.5% of the true capacities.

To see more clearly the comparison of the capacity predictions, Fig. 6 provides a close-up view of the far right side of Fig. 5. The three single discharge curves give normalized cell capacities of 0.9315, 0.9795 and 0.9916. This is to be compared to the predictions of the signature curve of 0.9463, 0.9831 and 0.9907 for these rates. The lowest-rate data points are accurately matched by the signature-curve discharge (not shown in the Figure). These experimental results are in complete agreement with the simulations presented earlier, including, for example, that the signature curve tends to predict a slightly higher attainable capacity when it is in error. However, it is apparent that the method gives a good prediction of the capacity with a great saving of time.

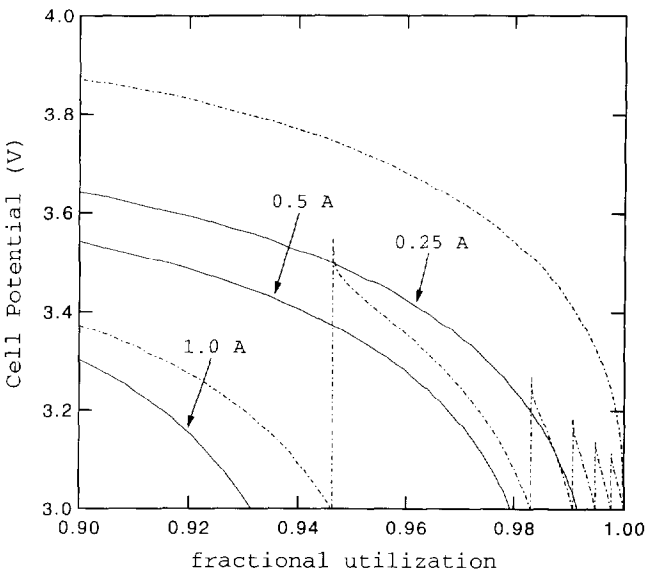

Fig. 6. Comparison of predicted capacity from a signature curve (dotted line) with that of three individual discharge curves (solid lines) at various rates. This Figure provides a closer view of Fig. 5 to emphasize the predictions of the signature curve. All data are taken from a Moli Energy test cell.

The simulations above have focused on the lithium–manganese-oxide spinel electrode, but generalization of these results is straightforward. The primary feature of a given insertion material that impacts the relaxation processes is the slope of the open-circuit potential (dU/dy). If the slope is appreciable, then the current distribution in the porous electrode should be uniform, and material redistribution processes can safely be ignored. Thus, for materials such as TiS_2 or petroleum cokes the choice of an optimum relaxation time is not important. However, if the open-circuit potential is fairly flat or stepped with flat regions, like the manganese-oxide spinel, then one can expect a non-uniform current distribution and thus non-uniform material utilization. Insertion materials with stepped open-circuit potential functions (Mn_2O_4, vanadium oxides, graphites, etc.) can be expected to have complicated redistribution processes occurring during relaxation; these materials are then the most sensitive to the choice of relaxation time.

Thus, the issue of the optimum relaxation time involves a balance between wanting some relaxation of lithium in the active material and concentration gradients to occur while not allowing sufficient time for the complete redistribution of lithium to a uniform state. Ideally, one would want the situation at the beginning of a discharge step to be identical to that which would exist if one had discharged directly to that point using the given discharge rate (instead of the higher rate that was actually used). This implies that concentration gradients will be too large and the material utilization profile will be too non-uniform after each current interruption. Although we cannot possibly hope to obtain the proper distributions of lithium in the active material during the relaxation processes, we can satisfy the compromise stated above by using a relaxation time which is less than the time constant for the active material redistribution process. The optimum time identified from the simulations above was approximately 5 min; however, this will obviously vary somewhat depending on the system parameters that impact the time constant for material redistribution.

An efficient and reliable method for measuring the capacity of a cell as a function of discharge rate is thus to use about seven, widely spaced discharges each followed by a 5 min relaxation period. The errors in the predicted capacities from Fig. 2 when using this procedure are less than 0.5%. The discharge rates should be chosen such that they cover the whole range of capacities, which guarantees that the full capacity versus rate curve will be obtained. It is safest to use fewer points at the higher discharge rates when the capacity is more sensitive to relaxation phenomena. More points at lower discharge rates do not adversely affect the validity of the results. One could, for example,

space the discharge rates uniformly on a logarithmic plot, as was done in Fig. 2.

6. List of symbols

c	concentration of electrolyte (mol dm^{-3})
D, D_s	diffusion coefficient of electrolyte and of lithium in the solid matrix (cm^2 s^{-1})
F	Faraday's constant, 96 487 (C/eq)
i_0	exchange current density (mA cm^{-2})
I	superficial current density (mA cm^{-2})
L	thickness of cell (m)
M	molar mass (g mol^{-1})
R	universal gas constant, 8.3143 (J mol^{-1} K^{-1})
R_s	radius of solid particles (m)
t_i^0	transference number of species i
T	temperature (K)
U	open-circuit potential (V)
V	cell potential (V)
x	stoichiometric coefficient of lithium in carbon, defined by Li_xC_6
y	stoichiometric coefficient of lithium in manganese oxide, defined by $Li_yMn_2O_4$

Greek letters

α_a, α_c	transfer coefficients
δ	thickness (m)
ϵ	porosity
κ	conductivity of electrolyte (S cm^{-1})
ρ	density (g cm^{-3})
σ	conductivity of solid matrix (S cm^{-1})
τ	time constant (s)

Subscripts

e	electrolyte
f	filler
s	solid phase or separator
t	concentration in insertion material for $y=1$
+	positive electrode
−	negative electrode

Superscripts

0	initial condition

Acknowledgements

We gratefully acknowledge the assistance of Ulrich von Sacken from Moli Energy and Jeff Dahn from Simon Frazer University who first suggested this project. This work was supported, in part, by the Assistant Secretary for Energy Efficiency and Renewable Energy, Office of Transportation Technologies, Electric and Hybrid Propulsion Division of the US Department of Energy under Contract No. DE-AC03-76SF00098.

Appendix A

Transport properties of the electrolyte and thermodynamic data

1. Propylene carbonate, 1 M $LiClO_4$

The concentration dependence of the conductivity was fit from available data of Gores and Barthel [7]. The diffusion coefficient of the salt [8] ($D=2.58\times10^{-6}$ cm^2 s^{-1}) and transference number of lithium [9] ($t_+^0=0.2$) were taken to be constant, since reproducible data were not available on their concentration dependence. Activity coefficient data have not been reported.

2. Electrode thermodynamic data

The open-circuit potential versus state-of-charge for the lithium–manganese-oxide spinel [10] was fit to the function:

$$U=4.06279+0.0677504\tanh[-21.8502y+12.8268]-0.105734\left[\frac{1}{(1.00167-y)^{0.379571}}-1.576\right]-0.045\exp(-71.69y^8)+0.01\exp[-200(y-0.19)] \quad \text{(A1)}$$

where y is the amount of lithium inserted in $Li_yMn_2O_4$. Similarly, for the carbon electrode [11]:

$$U=-0.132+1.41\exp(-3.52x) \quad \text{(A2)}$$

where x is the value defined by the formula Li_xC_6.

References

[1] M. Doyle, T.F. Fuller and J. Newman, *J. Electrochem. Soc., 140* (1993) 1526.
[2] T.F. Fuller, M. Doyle and J. Newman, *J. Electrochem. Soc., 141* (1994) 1.
[3] M. Doyle, T.F. Fuller and J. Newman, *Electrochim. Acta, 39* (1994) 2073.
[4] D. Guyomard and J.M. Tarascon, *J. Electrochem. Soc., 139* (1992) 937.
[5] J.M. Tarascon, D. Guyomard and G.L. Baker, *J. Power Sources, 43/44* (1993) 689.
[6] T.F. Fuller, M. Doyle and J. Newman, *J. Electrochem. Soc., 141* (1994) 982.
[7] H.J. Gores and J. Barthel, *J. Solution Chem., 9* (1980) 939.
[8] J.M. Sullivan, D.C. Hanson and R. Keller, *J. Electrochem. Soc., 117* (1970) 779.
[9] K. West, T. Jacobsen and S. Atlung, *J. Electrochem. Soc., 129* (1982) 1480.
[10] T. Ohzuku, M. Kitagawa and T. Hirai, *J. Electrochem. Soc., 137* (1990) 769.
[11] R. Fong, U. von Sacken and J.R. Dahn, *J. Electrochem. Soc., 137* (1990) 2009.